Research in Astron. Astrophys. **2009** Vol. **9** No. **2**, 213–219
http://www.raa-journal.org *http://www.iop.org/journals/raa*

***R**esearch in*
***A**stronomy and*
***A**strophysics*

X-ray plateaus followed by sharp drops in GRBs 060413, 060522, 060607A and 080330: Further evidences for central engine afterglow from gamma-ray bursts

Xiao-Hui Zhang

Department of Physics, Yunnan University, Kunming 650091, China; *xhzhang2008@yahoo.cn*

Received 2008 January 15; accepted 2008 May 19

Abstract The X-ray afterglows of GRBs 060413, 060522, 060607A and 080330 are characterized by a plateau followed by a very sharp drop. The plateau could be explained within the framework of the external forward shock model but the sharp drop can not. We interpret the plateau as the afterglows of magnetized central engines, plausibly magnetars. In this model, the X-ray afterglows are powered by the internal magnetic energy dissipation and the sudden drop is caused by the collapse of the magnetar. Accordingly, the X-ray plateau photons should have a high linear polarization, which can be tested by future X-ray polarimetry.

Key words: gamma-rays: bursts — ISM: jets and outflows — radiation mechanisms: non-thermal

1 INTRODUCTION

Gamma-Ray Bursts (GRBs) are by far the most luminous objects in the universe. They are bright flashes of high energy photons. A typical GRB usually lasts about several or tens of seconds. In the standard fireball model, the prompt γ-ray emission is powered by internal shocks (Paczynski & Xu 1994; Rees & Mészáros 1994; Kobayashi et al. 1997; Daigne & Mochkovitch 1998; Spruit et al. 2001; Fan, Wei & Zhang 2004), and the GRB afterglows are the emission of the external forward shock driven by the GRB fireball expanding into the surrounding medium (Mészáros & Rees 1997; Sari et al. 1998; Dai & Lu 1998a; Chevalier & Li 2000; Huang et al. 2000). The fireball afterglow model has been widely accepted because it works reasonably well by reproducing the late time multi-wavelength afterglow data in the pre-*Swift* era (e.g., Sari et al. 1998; Panaitescu & Kumar 2002; Piran 2004).

The GRB central engine may also play an important role in producing afterglow emission, i.e., the so-called "central engine afterglow" (Katz, Piran & Sari 1998; Fan, Piran & Xu 2006). One disadvantage of this model is its lack of predictive power. Though somewhat ad hoc, people began to interpret data with this model. For example, Piro et al. (1998) discovered a late-time outburst in the X-ray afterglow of GRB 970508 and attributed such an outburst to the re-activity of the central engine. However, the energy injection model can reproduce the multi-wavelength outburst data well (Panaitescu et al. 1998). The late time outburst detected in GRB 970508 is not a good *central engine afterglow* candidate. The situation changed dramatically in 2005. Piro et al. (2005) discovered two very early X-ray flares in GRB 011121, which had been interpreted as the central engine afterglow—the prompt emission powered by the re-activity of the central engine (Fan & Wei 2005). Since then, more and more X-ray flares have been well detected in early afterglows (e.g., Nousek et al. 2006; Burrows et al. 2005), and their central engine origin has been well established (e.g., Zhang et al. 2006).

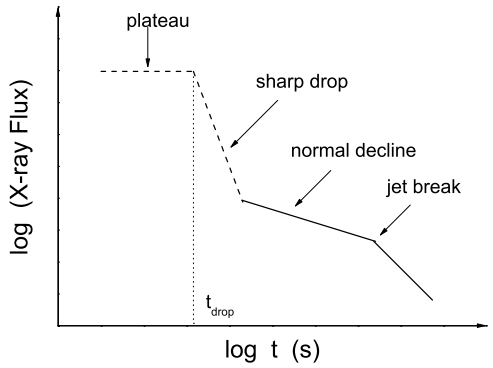

Fig. 1 The plateau followed by a sharp drop is another central engine afterglow.

In view of the similarity of the temporal behaviors of X-ray flares and GRBs, it is not a surprise to see that they have a common origin. Central engine afterglows may be more common than previously thought. People even discovered that some power-law decaying X-ray afterglows might have a central engine origin. A good example may be the afterglow of GRB 060218. As shown in Fan et al. (2006), the inconsistency of the X-ray afterglow flux with the radio afterglow flux and the very steep XRT spectra support the central engine afterglow hypothesis (see Zhang et al. 2007; Liang et al. 2007 for more cases). Recently, Troja et al. (2007) argued that the X-ray plateau is followed by a sharp drop in GRB 070110 is also a central engine afterglow.

In this work, we discuss the optical and X-ray afterglow of GRB 060607A. We show that not only the early X-ray plateau is followed by a sharp drop, but also the very early optical re-brightening may be due to the prompt emission of the long activity of the central engine. This result suggests that the central engine optical/X-ray afterglows might be common. We also apply the central engine afterglow model to a few more bursts, including GRB 060413, GRB 060522 and GRB 080330.

2 OBSERVATIONS

GRBs 060413, 060522, 060607A, 070110 and 080330 are different in many aspects, for example, their redshifts and the isotropic energies of the prompt γ-ray emission (Molinari et al. 2007; Liang et al. 2007; Tueller et al. 2006; Ledoux et al. 2006). However, their X-ray afterglows share a common character. As schematically plotted in Figure 1, an X-ray flat segment with a luminosity of $L_{\rm x} \sim 10^{47} - 10^{48}\,{\rm erg\,s^{-1}}$ is evident in the early afterglow phase (see Table 1 for details). The plateau disappeared suddenly with a decline as steep as t^{-4} or even t^{-8}. The optical afterglow of GRB 060607A is characterized by an optical flare hidden in the first optical re-brightening. The optical flare drops with time as t^{-11} (see fig. 2 of Nysewander et al. 2007). These peculiar behaviors are inconsistent with the regular afterglow model and may shed some light on the central engine.

3 INTERPRETATION OF THE DATA

A few physical processes are able to give rise to an X-ray flat segment. Below, we discuss three of them, including the energy injection model, the density jump model and the central engine afterglow model.

3.1 Energy Injection Model

We assume that the GRB central engine does not die after the prompt γ-ray emission. Such a long living central engine has an energy output $L \propto t^{-q}$ (Cohen & Piran 1999; Zhang & Mészáros 2001), where

$q \geq 1$ represents the weak energy injection and $q = 0$ corresponds to the early time energy injection from a fast rotating pulsar/magnetar (Dai & Lu 1998b; Zhang & Mészáros 2001; Dai 2004; Fan & Xu 2006). Other q values are possible if an energy injection results from slower material progressively catching up (viz. the Lorentz factor of a GRB has a wide range) (Rees & Mészáros 1998; Kumar & Piran 2000) or if an energy injection is caused by the fall-back of the envelope of the massive star (MacFadyen, Woosley & Heger 2001).

If the energy injection is significant enough to modify the dynamics of the forward shock, the afterglow light curves will also be modified (Zhang et al. 2006). For the X-ray plateau, $\nu > \max\{\nu_c, \nu_m\}$ is usually satisfied, where ν is the observer's frequency, ν_c is the cooling frequency and ν_m is the typical forward shock synchrotron radiation frequency (Sari et al. 1998). Under this condition, the temporal decline index of the X-ray afterglow should be

$$\alpha = \frac{(2p-4)+(p+2)q}{4}, \tag{1}$$

where $p \sim 2.3$ is the energy distribution power-law index of the shocked electrons in the blast wave. In GRB 060607A, the decay of the plateau before the sharp drop can be approximated as $t^{-0.1}$. Taking $p \sim 2.3$, we have (note that now $\alpha \sim 0.1$)

$$q \sim 0,$$

which is consistent with a pulsar/magnetar energy injection. Similar conclusions can be drawn for X-ray flat segments that were also detected in GRBs 060403, 060522, 070110 and 080330.

In this model, the X-rays are the synchrotron radiation of electrons accelerated by the forward shock. Their decline is determined by the dynamics of the forward shock and by the spherical curvature of the blast wave. Usually the decline should be shallower than t^{-p} (see Piran 2004 and Zhang 2007 for reviews). With a typical $p \sim 2.3$, a decline shallower than $t^{-2.3}$ is not steep enough to account for the sharp drops detected in GRBs 060413, 060522, 060607A, 070110 and 080330 ($\alpha = 4 \sim 8$). Therefore, the energy injection model is not favored in these particular cases.

3.2 Density Jump Model

Dai & Lu (2002) proposed a density jump model to account for some afterglow re-brightening. In this model, if the density jump is large enough, strong reverse shock emissions form and will give rise to strong X-ray/UV/optical emissions (cf. Nakar & Granot 2007). The decline of the afterglow light curves will also be suppressed. Hence, it has the potential to account for the X-ray flat segments that were detected in GRBs 060413, 060522, 060607A, 070110 and 080330. However, currently the forward and reverse shock regions move with the same bulk Lorentz factor. The curvature effect of the reverse shock emission is the same as that of the forward shock emission. As shown in many studies (e.g., Fenimore et al. 1996; Kumar & Panaitescu 2000; Fan & Wei 2005; Zhang et al. 2006; Liang et al. 2006), because of the spherical curvature of the emitting region and because of the special relativity effect, the external forward shock emission cannot drop with time more quickly than

$$F_\nu \propto t^{-(2+\beta)}, \tag{2}$$

where β is the spectral index of the X-ray emission. The only exception is that the ejecta is so narrow that we have seen its edge. If true, the optical emission would show the same behavior, which is not the case. We then conclude that the density jump model is not a good candidate for interpreting the X-ray plateaus followed by sharp drops.

Recently, Nysewander et al. (2007) employed the density jump model to account for the optical re-brightening detected in GRB 060607A. We, however, find out that the first optical flare hidden in the re-brightening (see their fig. 2) has a very steep decline $\sim t^{-11}$, which seriously violates the curvature effect constraint. Therefore, such an interpretation is problematic.

3.3 Central Engine Afterglow Model

Some authors have discussed the energy injection of a pulsar/magnetar wind and its influence on the afterglow emission (Dai & Lu 1998b; Zhang & Mészáros 2001). Strong magnetic energy dissipation (e.g. via reconnection) may take place if the continued outflow from the central engine is Poynting-flux dominated (Fan, Zhang & Proga 2005; Gao & Fan 2006; Giannios 2006), as happened in the prompt γ-ray emission phase (Usov 1994; Thompson 1994; Lyutikov & Blandford 2003). In this case, part of the magnetic energy of the outflow will be converted into the delayed prompt emission, maybe mainly in X-ray band, before they are injected into the forward shock.

Here, following Gao & Fan (2006) and Troja et al. (2007), we discuss the central engine afterglow powered by a millisecond magnetar. It is well known that the spin-down timescale of a millisecond magnetar can be estimated as

$$T_{\rm em} = 4\times10^3\ {\rm s}\ (1+z) I_{45.3} B_{p,15}^{-2} P_{0,-3}^2 R_{\rm s,6}^{-6}, \tag{3}$$

where $B_{p,15} = B_p/10^{15}$ Gauss is the magnetic field of dipole radiation of the pulsar in units of 10^{15} Gauss, $P_{0,-3}$ is the initial rotation period in milliseconds, $I_{45.3}$ is moment of inertia in units of 2×10^{45} g cm^2 and $R_{\rm s,6}$ is the stellar radius in units of 10^6 cm.

The dipole radiation luminosity is

$$L_{\rm dip} \approx 10^{49}\ {\rm erg\ s^{-1}}\ B_{\rm p,15}^2 R_6^6 P_{0,-3}^{-4} \Big[1+\frac{t}{T_{\rm em}}\Big]^{-2}. \tag{4}$$

We have $L_{\rm dip}\propto t^0$ for $t\ll T_{\rm em}$ and $L_{\rm dip}\propto t^{-2}$ for $t\gg T_{\rm em}$.

For such a Poynting-flux-dominated flow, the dissipation of the magnetic fields may produce X-ray/γ-ray emission (Usov 1994; Zhang & Mészáros 2002; Fan et al. 2005). In this work, we adopt the so-called MHD approximation breakdown model (Usov 1994). By comparing the pair density ($\propto r^{-2}$, r is the radial distance from the central source) with the density required for co-rotation ($\propto r^{-1}$ beyond the light cylinder of the compact object), one can estimate the radius $r_{\rm MHD}$ at which the MHD condition breaks down $r_{\rm MHD}\sim(2\times10^{15}) L_{\rm dip,48}^{1/2}\sigma_1^{-1} t_{v,m,-3}\Gamma_2^{-1}$ cm (e.g. Zhang & Mészáros 2002; Fan et al. 2005), where σ is the ratio of the magnetic energy flux to the particle energy flux, $t_{v,m}$ is the minimum variability timescale of the central engine and Γ is the bulk Lorentz factor of the outflow. Beyond this radius, intense electromagnetic waves are generated and outflowing particles are accelerated (Usov 1994). This converts magnetic energy into radiation. At $r_{\rm MHD}$, the comoving magnetic fields $B_{\rm MHD}$ can be estimated as $B_{\rm MHD}\sim 50\ \sigma_1 t_{v,m,-3}^{-1}$ Gauss. At $r_{\rm MHD}$, the typical synchrotron radiation frequency of the accelerated electrons can be estimated as (Fan et al. 2005)

$$\nu_{\rm m,MHD}\sim 6\times10^{16}\sigma_1^3 C_p^2\Gamma_2 t_{v,m-3}(1+z)^{-1}\ {\rm Hz}, \tag{5}$$

where $C_p\equiv(\frac{\epsilon_e}{0.5})[\frac{13(p-2)}{3(p-1)}]$, ϵ_e is the fraction of the dissipated comoving magnetic field energy converted to the comoving kinetic energy of the electrons, and the accelerated electrons distribute as a single power-law $dn/d\gamma_e\propto\gamma_e^{-p}$. According to this model, a σ much larger than 10 is not favored.

The cooling Lorentz factor of the accelerated-electrons can be generally estimated as $\gamma_{\rm e,c}\sim 4.5\times10^{19}\Gamma/(r_{\rm MHD}B^2)$, which is $\sim 10^3$ for typical parameters taken here and is comparable to $\gamma_{\rm e,m}$. The synchrotron radiation of the accelerated electrons peaks in the soft X-ray band. The energy emitted in the X-ray band is just a fraction ($\epsilon_{\rm x}$) of the total magnetic energy dissipated, so we have

$$L_{\rm x}\sim\epsilon_{\rm x}L_{\rm dip}\sim 10^{48}\ {\rm erg\ s^{-1}}\ \epsilon_{\rm x,-1} B_{\rm p,15}^2 R_6^6 P_{0,-3}^{-4}\Big[1+\frac{t}{T_{\rm em}}\Big]^{-2}. \tag{6}$$

We now have a set of free parameters $(B_{\rm p}, P_0, I, R_{\rm s}, \epsilon_{\rm x})$, however, just two of the observation data, $L_{\rm x}$ and the sharp drop time

$$t_{\rm drop}\sim fT_{\rm em}\sim 4\times10^3\ {\rm s}\ (1+z) f I_{45.3} B_{p,15}^{-2} P_{0,-3}^2 R_{\rm s,6}^{-6}, \tag{7}$$

where f is also a free parameter. Therefore, these free parameters can be fully determined by the limited observation data. We fix $(B_{\rm p}, P_0, I, R_{\rm s})$ with the typical values $\sim (10^{15}\ {\rm Gauss}, 1\,{\rm ms}, 2\times 10^{45}{\rm g\ cm^2}, 10^6{\rm cm})$ and then constrain $\epsilon_{\rm x}$ and f, respectively. The results are shown in Table 1. We do not want to over-interpret the results because the typical values of $(B_{\rm p}, P_0, I, R_{\rm s})$ adopted here might be biased, as are the derived $\epsilon_{\rm x}$ and f. For GRB 060413, GRB 060607A and GRB 070110, the parameters are largely reasonable and thus support the millisecond magnetar central engine hypothesis. For GRB 060522 and GRB 080330, $E_{\rm x}\approx t_{\rm drop}L_{\rm x}/(1+z)\sim 10^{50}$ erg is significantly smaller than the total rotational energy of a millisecond magnetar $\sim I(2\pi/P_0)^2/2\sim 4\times 10^{52}I_{45.3}P_{0,-3}^{-2}$ erg. Possibly these two magnetars were hypermassive and collapsed before losing a significant fraction of the rotational energy and angular momentum (Fan & Xu 2006). Alternatively, the magnetic field of the magnetars decayed suddenly for some unknown reasons (Troja et al. 2007). The current data are not sufficient for us to distinguish between these two possibilities. In the future, a gravitational wave observation may shed some light on the nature of the X-ray drop because the collapse of the hypermassive magnetar may give rise to interesting gravitational signals.

Table 1 Fit of the central engine afterglows of several GRBs, where B_p, R_s, I and P_0 are fixed.

GRBs	$t_{\rm drop}$(s)	z	$L_{\rm x}$(erg s^{-1})	$\epsilon_{\rm x}$	f	$F_{\nu_{\rm v}}/F_{\nu_{\rm x}}$
GRB 060413	2×10^4	3	1.02×10^{48}	0.4	1.2	3.4
GRB 060522	4×10^2	5.11	2.48×10^{48}	0.2	0.02	5.2
GRB 060607A	1.5×10^4	3.08	1.71×10^{48}	0.4	0.9	10
GRB 070110	2×10^4	2.35	2.7×10^{47}	0.1	1.4	1.4
GRB 080330	1.0×10^3	1.51	1.12×10^{47}	0.01	0.1	62

Reference: *http://www.swift.ac.uk/*, Liang et al. (2007), Troja et al. (2007).
Notes: For GRB 060413 we set $z\sim 3$, the typical redshift of Swift GRBs.

The prolonged activity of the central engine should also produce some emission in the optical band. A simple estimate is the following. The synchrotron self-absorption frequency can be estimated as (e.g., Fan & Wei 2005)

$$\nu_{\rm a}\sim 2\times10^{14}\ {\rm Hz}\ [2/(1+z)]^{3/7}L_{\rm dip,48}^{2/7}\Gamma_2^{3/7}r_{\rm MHD,15}^{-4/7}B_{\rm MHD,2}^{1/7}\,, \tag{8}$$

which is below the optical band $\nu_{\rm v}\sim 5\times10^{14}$ Hz. With $\gamma_{\rm e,m}\sim\gamma_{\rm e,c}$ and $\nu_{\rm m,MHD}\sim\nu_{\rm x}\sim 7.2\times10^{16}$ Hz, the optical central engine afterglow flux is not expected to be dimmer than

$$F_{\nu_{\rm v}}\sim F_{\nu_{\rm x}}(\nu_{\rm v}/\nu_{\rm x})^{1/3}\sim 0.2F_{\nu_{\rm x}}\,. \tag{9}$$

Consequently, the observed optical emission should be brighter than $\sim 0.2F_{\nu_{\rm x}}$, which is consistent with the observations, as shown in Table 1.

4 DISCUSSION AND CONCLUSIONS

In contrast to what was believed in the pre-*Swift* era, it is evident now that the central engine plays an important role in producing afterglow emission (see Fan, Piran & Wei 2008 for a review). Most theoretical works so far focus on the energetic flares that are well detected in many *Swift* GRBs. The temporal behavior of the flaring X-rays are quite similar to that of the prompt γ-rays. It is thus reasonable that the flares and the prompt GRB have a common origin. In this work, we show that the X-ray plateaus followed by sharp drops detected in GRBs 060413, 060522, 060607A, 070110 and 080330 are also good candidates for the so-called "*central engine afterglow*" (see also Jin & Fan 2007; Troja et al. 2007; Staff et al. 2007). The energy injection model and the density jump model are less favored. We also find out that both the luminosity and the timescale of the X-ray plateaus detected in GRBs 060413, 060522 and 070110 are consistent with the central engine afterglow emission powered by millisecond magnetars (see Section 3.3 for details). For GRB 060522 and GRB 080330, the X-ray drop appeared so early that

it might suggest that the two magnetars, if they were, had collapsed before losing a significant part of their rotational energies and angular momenta. Although millisecond magnetars are believed to be natural outcomes of the collapse of massive stars, the identification of this kind of compact object at cosmological distances is not easy. Fairly speaking, an additional independent signature, like a high linear polarization (see Fan, Xu & Wei 2008), is needed before the magnetar wind dissipation model for the X-ray plateaus that are followed by X-ray drops can be generally accepted.

Acknowledgements I thank the anonymous referee for insightful comments, and Prof. L. Zhang and Dr. Y. Z. Fan for their kind help.

References

Burrows, D. N., et al. 2005, Science, 309, 1833
Chevalier, R. A., & Li, Z. Y. 2000, ApJ, 536, 195
Cohen, E., & Piran, T. 1999, ApJ, 518, 346
Dai, Z. G. 2004, ApJ, 606, 1000
Dai, Z. G., & Lu, T. 1998a, MNRAS, 298, 87
Dai, Z. G., & Lu, T. 1998b, A&A, 333, L87
Dai, Z. G., & Lu, T. 2002, ApJ, 565, L87
Daigne, F., & Mochkovitch, R. 1998 MNRAS, 296, 275
Fan, Y. Z., Piran, T., & Wei, D. M. 2008, AIPC, 968, 32
Fan, Y. Z., Piran, T., & Xu, D. 2006, JCAP, 09, 013
Fan, Y. Z., & Xu, D. 2006, MNRAS, 372, L19
Fan, Y.-Z., Xu, D., & Wei, D.-M. 2008, MNRAS, 387, 92
Fan, Y. Z., & Wei, D. M. 2005, MNRAS, 364, L42
Fan, Y. Z., Wei, D. M., & Zhang, B. 2004, MNRAS, 354, 1031
Fan, Y. Z., Zhang, B., & Proga, D. 2005, ApJ, 635, L129
Fenimore, E. E., Madras, C. D., & Nayakshin, S. 1996, ApJ, 473, 998
Giannios, D. 2006, A&A, 455, L5
Gao, W. H., & Fan, Y. Z. 2006, ChJAA (Chin. J. Astron. Astrophys.), 6, 513
Huang, Y. F., Gou, L. J., Dai, Z. G., & Lu, T. 2000, ApJ, 543, 90
Jin, Z. P., & Fan, Y. Z. 2007, MNRAS, 378, 1043
Kumar, P., & Panaitescu, A. 2000, ApJ, 541, L51
Kumar, P., & Piran, T. 2000, ApJ, 532, 286
Katz, J. I., Piran, T., & Sari, R. 1998, Phys. Rev. Lett., 80, 1580
Kobayashi, S., Piran, T., & Sari, R. 1997, ApJ, 490, 92
Ledoux, C., Vreeswijk, P., Smette, A., et al. 2006, GCN Circ, 5237
Liang, E. W., Zhang, B., O'Brien, P. T., et al. 2006, ApJ, 646, 351
Liang, E. W., Zhang, B. B., & Zhang, B. 2007, ApJ, 670, 565
Lyutikov, M., & Blandford, R. 2003, arXiv: astro-ph/0312347
MacFadyen, A. I., Woosley, S. E., & Heger, A. 2001, ApJ, 550, 410
Mészáros, P., & Rees, M. J. 1997, ApJ, 476, 232
Molinari, E., Vergani, S. D., Malesani, D., et al. 2007, A&A, 469, L13
Nakar, E., & Granot, J. 2007, MNRAS, 380, 1744
Nousek, J. A., Kouveliotou, C., Grupe, D., et al. 2006, ApJ, 642, 389
Nysewander, M., Reichzrt, D. E., Crain, J. A., et al. 2007, arXiv:0708.3444
Paczynski, B., & Xu, G. 1994, ApJ, 427, 708
Panaitescu, A., & Kumar, P. 2002, ApJ, 571, 779
Panaitescu, A., Meszaros, P., & Rees, M. J. 1998, ApJ, 503, 314
Piro, L., Amati L., Antonelli, L. A., et al. 1998, A&A, 331, L41
Piro, L., De Pasquale, M., Soffitta, P., et al. 2005, ApJ, 623, 314
Piran, T. 2005, Reviews of Modern Physics, 76, 1143
Rees, M. J., & Mészáros, P. 1994, ApJ, 430, L93

Rees, M. J., & Mészáros, P. 1998, ApJ, 496, L1
Sari R., Piran T., & Narayan, R. 1998, ApJ, 497, L17
Spruit, H. C., Daigne, F., & Drenkhahn, G. 2001, A&A, 369, 694
Staff, J., Niebergal, B., & Ouyed, R. 2008, MNRAS, 391, 178
Thompson, C. 1994, MNRAS, 270, 480
Troja, E., Cusumano, G., O'Brien P. T., et al. 2007, ApJ, 665, 599
Tueller, J., Barbier, L., Barthelmy, S., et al. 2006, GCN Circ, 5242
Usov, V. V. 1994, MNRAS, 267, 1035
Zhang, B. 2007, ChJAA (Chin. J. Astron. Astrophys.), 7, 1
Zhang, B., & Mészáros, P. 2001, ApJ, 552, L35
Zhang, B. Mészáros, P. 2002, ApJ, 566, 712
Zhang, B., Fan, Y. Z., & Dyks, J., et al. 2006, ApJ, 642, 354
Zhang, B. B., Liang, E. W., & Zhang, B. 2007, ApJ, 666, 1002